AVR495: AC Induction Motor Control Using the Constant V/f Principle and a Space-vector PWM Algorithm

AVR Microcontrollers

Application Note

1. Features

- Cost-effective and energy efficient 3-phase induction motor drive
- Interrupt driven
- Low memory and computing requirements

2. Introduction

In a previous application note [AVR494], the implementation on an AT90PWM3 of an induction motor speed control loop using the constant Volts per Hertz principle and a natural pulse-width modulation (PWM) technique was described. A more sophisticated approach using a space vector PWM instead of the natural PWM technique is known to provide lower energy consumption and improved transient responses. The aim of this application note is to show that this approach, though more computationally intensive, can also be implemented on an AT90PWM3.

3. AT90PWM3 Key Features

The control algorithms have been implemented on the AT90PWM3, a low-cost low-power single-chip microcontroller, achieving up to 16 MIPS and suitable for the control of DC-DC buck-boost converters, permanent magnet synchronous machines, three-phase induction motors and brushless DC motors. This device integrates:

- **8-bit AVR advanced RISC architecture microcontroller (core similar to the ATmega 88)**
- **8K Bytes of In-System-Programmable Flash memory**
- **512 Bytes of static RAM to store variables and lookup tables dedicated to the application program**
- **512 bytes of EEPROM to store configuration data and look-up tables**
- **one 8-bit timer and one 16-bit timer**
- **6 PWM channels optimized for Half-Bridge Power Control**
- **an 11-channel 10-bit ADC and a 10-bit DAC**
- **3 on-chip comparators**
- **a programmable watchdog timer with an internal oscillator**

7546A–AVR–12/05

4. Theory of Operation

4.1 Principle of the Space-Vector Modulation

Figure 4-1. Typical structure of an inverter-fed induction motor.

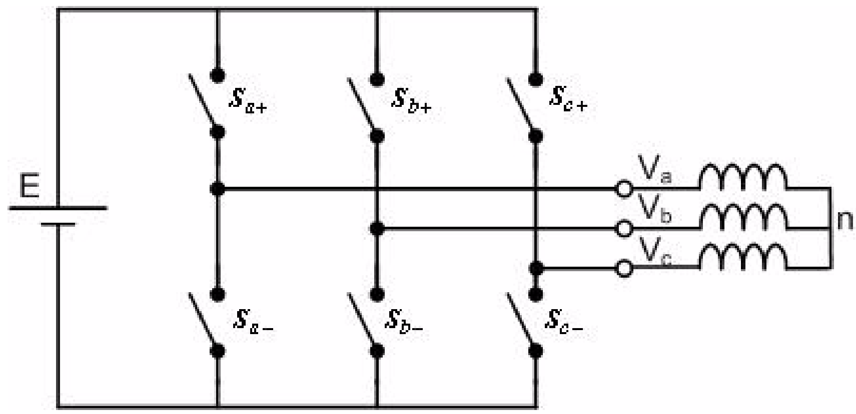

Figure 4-1.shows the typical structure of a three-phase induction motor connected to a VSI (Voltage Source Inverter). Since the motor is considered as a balanced load with an unconnected neutral, $V_n = \langle V_a + V_b + V_c \rangle / 3$, $V_{an} = V_a - V_n = (V_{ab} - V_{ca})/3$, $V_{bn} = V_b - V_n = (V_{bc} - V_{ab})/3$ and $V_{cn} = V_c - V_n = (V_{ca} - V_{bc})/3$. Since the upper power switches can only be On or Off, and since the lower ones are supposed to always be in the opposed state (the dead-times of the inverter legs are neglected), there are only eight possible switching states, as shown on Figure 4-2. Six of them lead to non-zero phase voltages, and two interchangeable states lead to zero phase voltages. When mapped in a 2D-frame fixed to the stator using a Concordia transformation [1,2], the six non-zero phase voltages form the vertices of a hexagon. (See Figure 4-3.)

$$\begin{bmatrix} V_\alpha \\ V_\beta \end{bmatrix} = \begin{bmatrix} 1 & -1/2 & -1/2 \\ 0 & \sqrt{3}/2 & -\sqrt{3}/2 \end{bmatrix} \begin{bmatrix} V_{an} \\ V_{bn} \\ V_{cn} \end{bmatrix}$$

Figure 4-2. Possible switching configurations of a 3-phase inverter

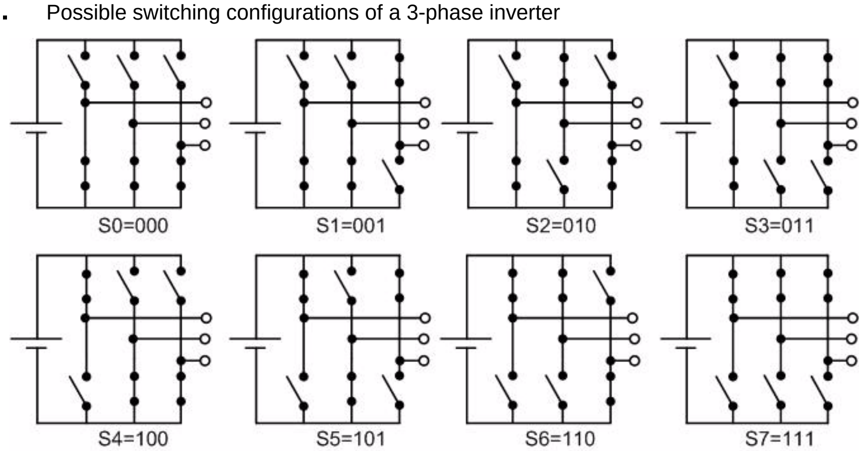

As shown on Figure 4-3., the angle between two successive non-zero voltages is always 60 degrees.

In complex form, these non-zero phase voltages can be written as $V_k = E\,e^{j(k-1)\frac{\pi}{3}}$, with k = 1..6 and $V_0 = V_7 = 0$ V. Table 4-1. shows the line-to-line and line-to-neutral voltages in each of the 8 possible configurations of the inverter.

Figure 4-3. Representation of the eight possible switching configurations in the Concordia reference frame

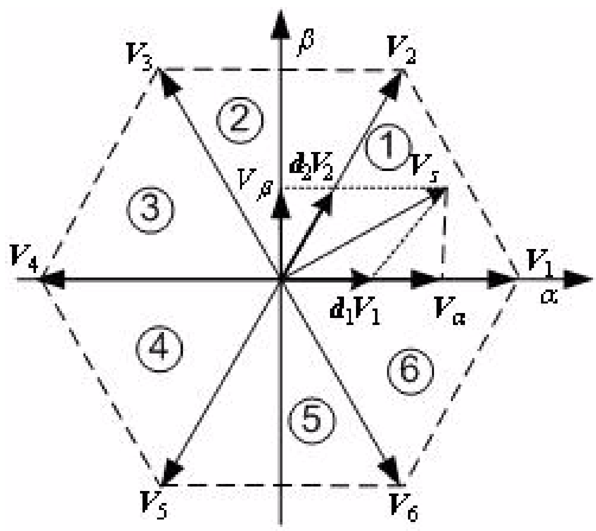

Table 4-1. Switching configurations and output voltages of a 3-phase inverter

S_{a+}	S_{b+}	S_{c+}	S_i	V_{ab}	V_{bc}	V_{ca}	V_{an}	V_{bn}	V_{cn}	V_α	V_β	V_i
0	0	0	S_0	0	0	0	0	0	0	0	0	V_0
0	0	1	S_1	0	-E	E	-E/3	-E/3	+2E/3	-E/2	$-E\sqrt{3}/2$	V_5
0	1	0	S_2	-E	E	0	-E/3	+2E/3	-E/3	-E/2	$E\sqrt{3}/2$	V_3
0	1	1	S_3	-E	0	E	-2E/3	-E/3	-E/3	-E	0	V_4
1	0	0	S_4	E	0	-E	+2E/3	-E/3	-E/3	E	0	V_1
1	0	1	S_5	E	-E	0	E/3	-2E/3	E/3	E/2	$-E\sqrt{3}/2$	V_6
1	1	0	S_6	0	E	-E	E/3	E/3	-2E/3	E/2	$E\sqrt{3}/2$	V_2
1	1	1	S_7	0	0	0	0	0	0	0	0	V_7

Table 4-2. Expressions of the duty cycles in each sector

Sector Number	θ	d_k	d_{k+1}
1	$\left[0, \frac{\pi}{3}\right]$	$\frac{2}{\sqrt{3}}\frac{V_s}{E}\sin(\frac{\pi}{3}-\theta)$	$\frac{2}{\sqrt{3}}\frac{V_s}{E}\sin(\theta)$
2	$\left[\frac{\pi}{3}, \frac{2\pi}{3}\right]$	$\frac{2}{\sqrt{3}}\frac{V_s}{E}\sin(\frac{\pi}{3}+\theta)$	$\frac{2}{\sqrt{3}}\frac{V_s}{E}\sin(\frac{5\pi}{3}+\theta)$
3	$\left[\frac{2\pi}{3}, \pi\right]$	$\frac{2}{\sqrt{3}}\frac{V_s}{E}\sin(\theta)$	$\frac{2}{\sqrt{3}}\frac{V_s}{E}\sin(\frac{4\pi}{3}+\theta)$
4	$\left[\pi, \frac{4\pi}{3}\right]$	$\frac{2}{\sqrt{3}}\frac{V_s}{E}\sin(\frac{5\pi}{3}+\theta)$	$\frac{2}{\sqrt{3}}\frac{V_s}{E}\sin(2\pi-\theta)$
5	$\left[\frac{4\pi}{3}, \frac{5\pi}{3}\right]$	$\frac{2}{\sqrt{3}}\frac{V_s}{E}\sin(\frac{4\pi}{3}+\theta)$	$\frac{2}{\sqrt{3}}\frac{V_s}{E}\sin(\frac{2\pi}{3}+\theta)$
6	$\left[\frac{5\pi}{3}, 2\pi\right]$	$\frac{2}{\sqrt{3}}\frac{V_s}{E}\sin(2\pi-\theta)$	$\frac{2}{\sqrt{3}}\frac{V_s}{E}\sin(\frac{\pi}{3}+\theta)$

In the Concordia frame, any stator voltage $V_s = V_\alpha + jV_\beta = V_{sm}\cos(\theta) + jV_{sm}\sin(\theta)$ located inside this hexagon belongs to one of the six sectors, and can be expressed as a linear combination of the two non-zero phase voltages which delimit this sector: $V_s = d_k V_k + d_{k+1}V_{k+1}$. Equating $d_k V_k + d_{k+1}V_{k+1}$ to $V_{sm}\cos(\theta) + jV_{sm}\sin(\theta)$ in each sector leads to the expressions of the duty cycles shown in Table 4-2. Since the inverter cannot instantaneously generate V_s, the space-vector PWM principle consists in producing a T_s **-**periodic voltage whose average value equals V_s,by generating V_k during $T_k = d_k T_s$ and V_{k+1} during $T_{k+1} = d_{k+1}T_s$**.** Since $d_k + d_{k+1} \le 1$, these voltages must be completed over the switching period T_s by V_0 and/or V_7. Several solutions are possible [3,4], and the one which minimizes the total harmonic distorsion of the stator current consists in applying V_0 and V_7 during the same duration $T_0 = T_7 = \frac{1 - d_k - d_{k+1}}{2}T_s$. V_0 is equally applied at the beginning and at the end of the switching period, whereas V_7 is applied at the middle. As an illustration, the upper side of Figure 4-4. shows the waveforms obtained in sector 1.

4.2 Efficient Implementation of the SV-PWM

Table 4-2. seems to show that the duty cycles have different expressions in each sector. A thorough study of these expressions show that since $\sin(x) = \sin(\pi - x)$, all these duty cycles can be written in a unified way as $d_k = \frac{2V_{sm}}{E\sqrt{3}}\sin(\theta'')$ and $d_{k+1} = \frac{2V_{sm}}{E\sqrt{3}}\sin(\theta')$, with $\theta'' = \frac{\pi}{3} - \theta'$ and $\theta' = \theta - (k-1)\frac{\pi}{3}$. Since these expressions no longer depend on the sector number, they can be denoted as d_a and d_b. Since θ' is always between 0 and $\frac{\pi}{3}$, computing d_a and d_b requires a sine table for angles inside this interval only. This greatly reduces the amount of memory required to store this sine table.

The AT90PWM3 provides the 3 power stage controllers (PSC) to generate the switching waveforms computed from the Space Vector algorythms.

The counters will count from zero to a value corresponding to one half of the switching period (as shown on the lower side of Fig. 4), and then count down to zero. The values that must be stored in the three compare registers are given in Table 4-3.

Figure 4-4. Inverter switch waveforms and corresponding compare register values

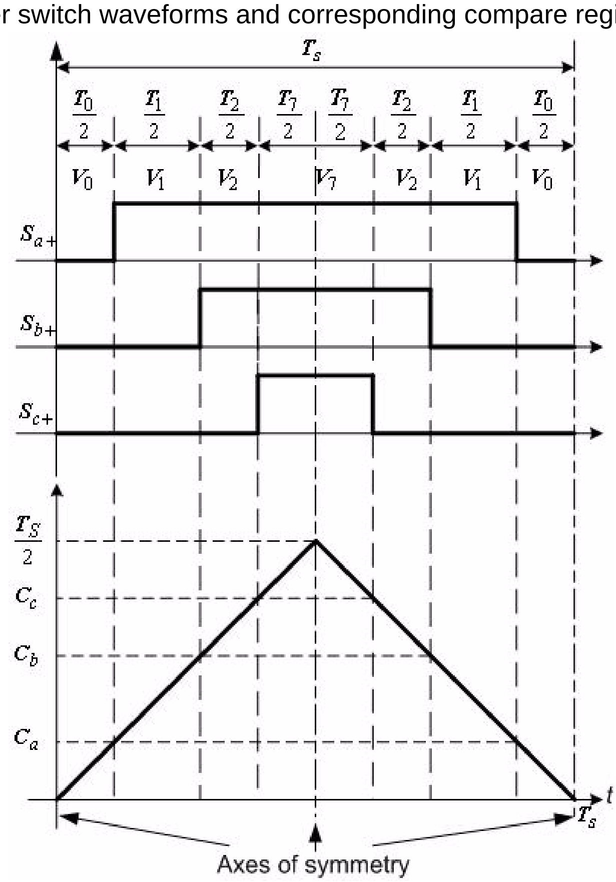

Table 4-3. Compare Register Values vs Sector Number

Sector Number	$\frac{4}{T_s}C_a - 1$	$\frac{4}{T_s}C_b - 1$	$\frac{4}{T_s}C_c - 1$
1	$-d_a - d_b$	$d_a - d_b$	$d_a + d_b$
2	$-d_a + d_b$	$-d_a - d_b$	$d_a + d_b$
3	$d_a + d_b$	$-d_a - d_b$	$d_a - d_b$
4	$d_a + d_b$	$-d_a + d_b$	$-d_a - d_b$
5	$d_a - d_b$	$d_a + d_b$	$-d_a - d_b$
6	$-d_a - d_b$	$d_a + d_b$	$-d_a + d_b$

4.3 Sector Determination Algorithm

To determine the sector which a given stator voltage V_s belongs to, some algorithms have been proposed in the literature which generally require many arithmetic operations and are based on the coordinates of V_s in the Concordia plane or in the a-b-c phase space. When this voltage is deduced from a V/f control principle, its modulus V_{sm} is computed by the V/f law recalled in the previous application note, and its phase θ is deduced from ω_s by a discrete-time integrator. To implement this sector determination algorithm efficiently, we manage θ' and k instead of θ in a dedicated integrator shown on Fig. 6. The sector number k is the output of a modulo six counter activated each time θ' exceeds $\frac{\pi}{3}$, and θ' is confined to lie between 0 and $\frac{\pi}{3}$ (see Fig. 7).

Figure 4-5. Sector determination algorithm

Initialization:

$\theta' = 0$; $\theta'' = \frac{\pi}{3}$; $k = 1$;

Beginning of the algorithm:

$\theta' = \theta' + \omega_s T_s$

if $\theta' \geq \frac{\pi}{3}$ **then**

$\theta' = \theta' - \frac{\pi}{3}$

if $k \geq 6$ **then** $k = 1$ **else** $k = k + 1$ **end**

end

$\theta'' = \frac{\pi}{3} - \theta'$

End of the algorithm

Figure 4-6. Sector determination

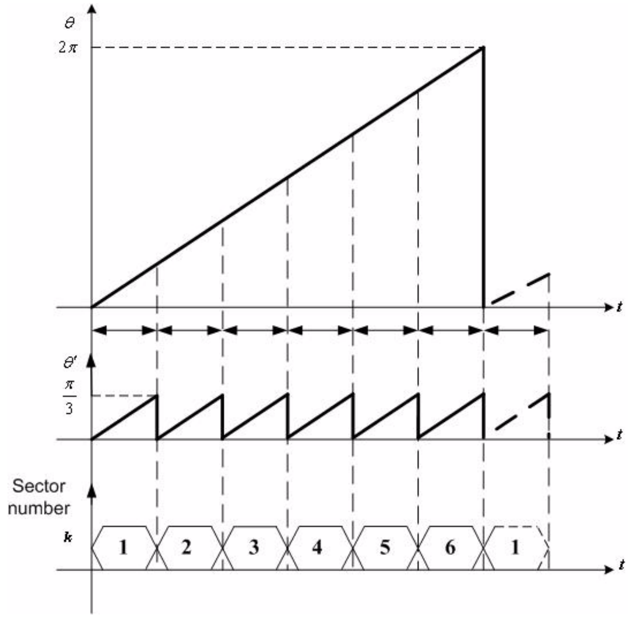

The resulting dataflow diagram, shown on Fig. 8, can be used to build a speed control loop (Figure 4-8.), in which the difference between the desired speed and the measured speed feeds a PI controller that determines the stator voltage frequency. To decrease the complexity of the controller, the input of the V/f law and of the space vector PWM algorithm is the absolute value of the stator voltage frequency. If the output of the PI controller is a negative number, two of the switching variables driving the power transistors of the inverter are interchanged.

Figure 4-7. Space Vector PWM data flow diagram

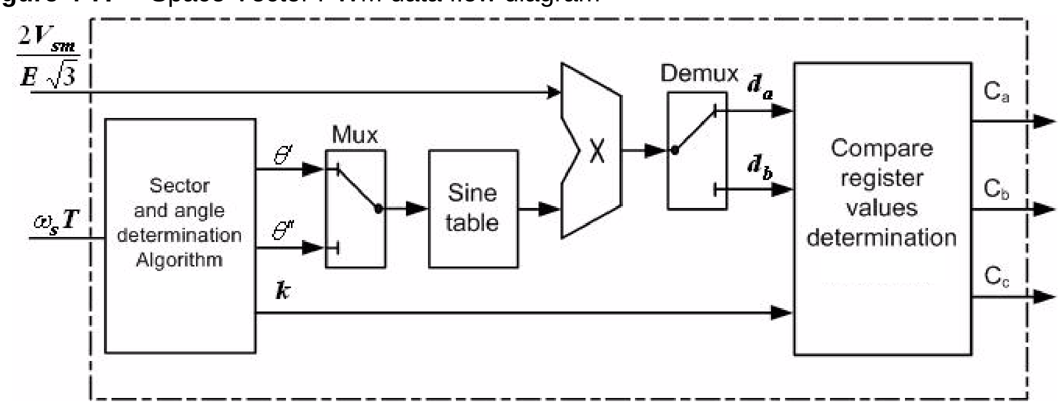

Figure 4-8. Block diagram of the complete control system.

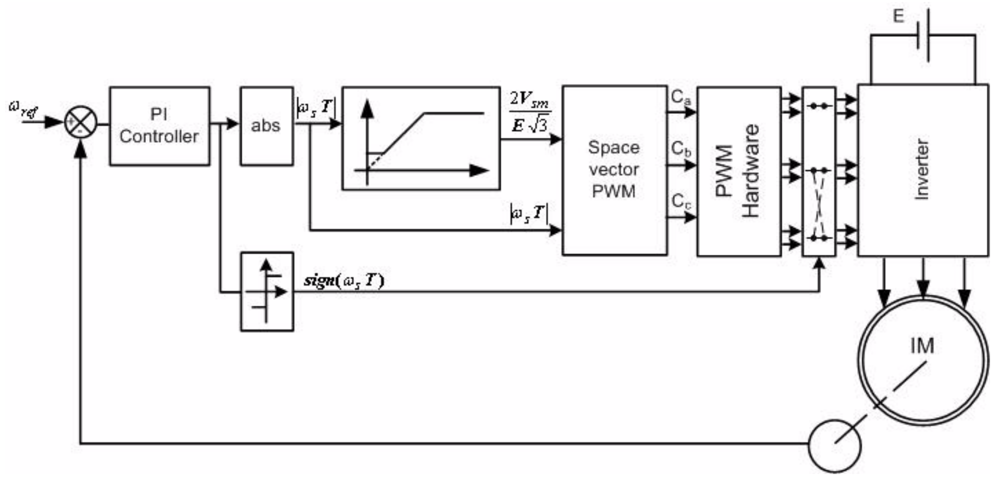

5. Hardware Description (ATAVRMC200)

This application is available on the ATAVRMC200 evaluation board. This board provides a way to start and experiment asynchronous motor control.

ATAVRMC200 main features:

- AT90PWM3 microcontroller
- 110-230VAC motor drive
- Intelligent Power Module (230V / 400W board sized)
- ISP & Emulator interface
- RS232 interface
- Isolated I/O for sensors
- 0-10V input for command or sensor

6. Software Description

All algorithms have been written in the C language using IAR's embedded workbench and AVR Studio as development tools. For the space vector PWM algorithm, a table of the rounded values of $127\sin(\frac{2\pi k}{480})$ for k between 0 and 80 is used. The length of this table (81 bytes) is a better trade-off between the size of the available internal memory and the quantification of the rotor shaft speed. For bi-directional speed control, the values stored in two of the comparators are interchanged when the output of the PI regulator is a negative number (see Figure 4-8.).

6.1 Project Description

The software is available in the attached project on the Atmel web Site. The project to use is Project_Vector. The Project_Natural corresponds to the AVR494 Application Note.

Table 6-1. List of Files used in the "Project_Vector".IAR project.

File	Description
main_space_vector_PWM.c	main upper level of the application
space_vector_PWM2.c	sector and theta determination
controlVF.c	Compute a constant V/F ratio
mc_control.c	regulation loop (PI)
read_acquisitionADC.c	return the ADC result
init.c	CPU initialization (IO ports, timers)
psc_initialisation2.c	PSC initialization
adc.c	ADC functions
dac.c	DAC functions

6.2 Experimentation

Figure 6-1. shows the speed response and the stator voltages obtained with the microcontroller for speed reference steps between +700 and -700 rpm. These experimental results were obtained with a 750 W induction machine. This figure shows that the desired speed is reached after a 1.2 s long transient, and that when the stator frequency ω_s obtained at the output of the PI regulator nears zero, the stator voltage magnitude is equal to the boost voltage. These figures also confirm that transient obtained with a a space vector PWM is smoother but also longer.

Figure 6-1. Measured speed (in rpm) and line-to-neutral stator voltage (in Volts) obtained with the microcontroller during speed reference steps

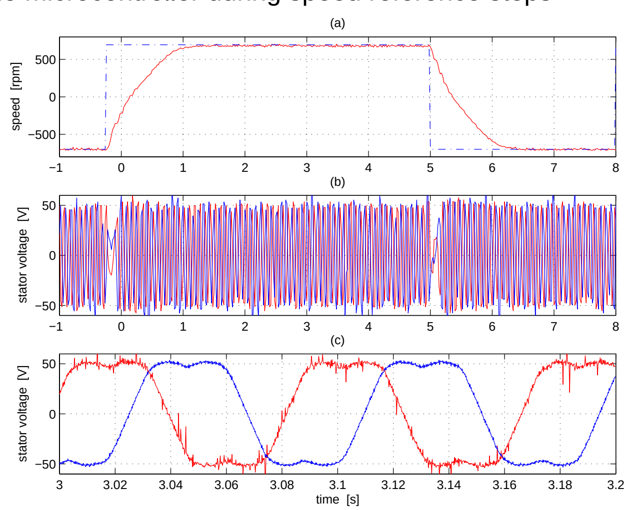

7. Resources

Code Size : 2 584 bytes

RAM Size : 217 bytes

CPU Load : 33% @ 8MHz

8. References

1. Atmel AVR494, AC Induction Motor Control Using the constant V/f Principle and a Natural PWM Algorithm.

2. W. Leonhard, “Control of electrical drives”, 2nd Ed, Springer, 1996.

3. F.A. Toliyat, S.G. Campbell, “DSP-based electromechanical motion control”, CRC Press, 2004.

4. Y.Y. Tzou, H.J. Hsu, “FPGA realisation of space-vector PWM control IC for three-phase PWM inverters”, IEEE Transactions on Power Electronics, Vol 12, No 6, pp 953-963, 1997.

5. K. Zhou, D. Wang, “Relation between space-vector modulation and three-phase carrier-based PWM”, IEEE Transactions on Industrial Electronics, Vol. 49, No. 1, pp 186-196, February 2002.

Atmel Corporation

2325 Orchard Parkway
San Jose, CA 95131, USA
Tel: 1(408) 441-0311
Fax: 1(408) 487-2600

Regional Headquarters

Europe
Atmel Sarl
Route des Arsenaux 41
Case Postale 80
CH-1705 Fribourg
Switzerland
Tel: (41) 26-426-5555
Fax: (41) 26-426-5500

Asia
Room 1219
Chinachem Golden Plaza
77 Mody Road Tsimshatsui
East Kowloon
Hong Kong
Tel: (852) 2721-9778
Fax: (852) 2722-1369

Japan
9F, Tonetsu Shinkawa Bldg.
1-24-8 Shinkawa
Chuo-ku, Tokyo 104-0033
Japan
Tel: (81) 3-3523-3551
Fax: (81) 3-3523-7581

Atmel Operations

Memory
2325 Orchard Parkway
San Jose, CA 95131, USA
Tel: 1(408) 441-0311
Fax: 1(408) 436-4314

Microcontrollers
2325 Orchard Parkway
San Jose, CA 95131, USA
Tel: 1(408) 441-0311
Fax: 1(408) 436-4314

La Chantrerie
BP 70602
44306 Nantes Cedex 3, France
Tel: (33) 2-40-18-18-18
Fax: (33) 2-40-18-19-60

ASIC/ASSP/Smart Cards
Zone Industrielle
13106 Rousset Cedex, France
Tel: (33) 4-42-53-60-00
Fax: (33) 4-42-53-60-01

1150 East Cheyenne Mtn. Blvd.
Colorado Springs, CO 80906, USA
Tel: 1(719) 576-3300
Fax: 1(719) 540-1759

Scottish Enterprise Technology Park
Maxwell Building
East Kilbride G75 0QR, Scotland
Tel: (44) 1355-803-000
Fax: (44) 1355-242-743

RF/Automotive
Theresienstrasse 2
Postfach 3535
74025 Heilbronn, Germany
Tel: (49) 71-31-67-0
Fax: (49) 71-31-67-2340

1150 East Cheyenne Mtn. Blvd.
Colorado Springs, CO 80906, USA
Tel: 1(719) 576-3300
Fax: 1(719) 540-1759

Biometrics/Imaging/Hi-Rel MPU/
High Speed Converters/RF Datacom
Avenue de Rochepleine
BP 123
38521 Saint-Egreve Cedex, France
Tel: (33) 4-76-58-30-00
Fax: (33) 4-76-58-34-80

Literature Requests
www.atmel.com/literature

7546A–AVR–12/05